

## Accepted Manuscript

Title: Synthesis and properties of a biodegradable polymer-drug conjugate: Methotrexate-poly(glycerol adipate)

Authors: Jiraphong Suksiriworapong, Vincenzo Taresco, Delyan P. Ivanov, Ioanna D. Styliari, Krisada Sakchaisri, Varaporn Buraphacheep Junyaprasert, Martin C. Garnett



PII: S0927-7765(18)30198-X  
DOI: <https://doi.org/10.1016/j.colsurfb.2018.03.048>  
Reference: COLSUB 9249

To appear in: *Colloids and Surfaces B: Biointerfaces*

Received date: 6-12-2017  
Revised date: 10-3-2018  
Accepted date: 27-3-2018

Please cite this article as: Jiraphong Suksiriworapong, Vincenzo Taresco, Delyan P.Ivanov, Ioanna D.Styliari, Krisada Sakchaisri, Varaporn Buraphacheep Junyaprasert, Martin C.Garnett, Synthesis and properties of a biodegradable polymer-drug conjugate: Methotrexate-poly(glycerol adipate), *Colloids and Surfaces B: Biointerfaces* <https://doi.org/10.1016/j.colsurfb.2018.03.048>

This is a PDF file of an unedited manuscript that has been accepted for publication. As a service to our customers we are providing this early version of the manuscript. The manuscript will undergo copyediting, typesetting, and review of the resulting proof before it is published in its final form. Please note that during the production process errors may be discovered which could affect the content, and all legal disclaimers that apply to the journal pertain.

**Synthesis and properties of a biodegradable polymer-drug conjugate: Methotrexate-poly(glycerol adipate)**

Jiraphong Suksiriworapong,<sup>\*,a,b</sup> Vincenzo Taresco,<sup>c</sup> Delyan P. Ivanov,<sup>d</sup> Ioanna D. Styliari,<sup>c,1</sup>

Krisada Sakchaisri,<sup>e</sup> Varaporn Buraphacheep Junyaprasert,<sup>a,b</sup> Martin C. Garnett<sup>c</sup>

<sup>a</sup>Department of Pharmacy, Faculty of Pharmacy, Mahidol University, Ratchathewi, Bangkok 10400, Thailand

<sup>b</sup>Center of Excellence in Innovative Drug Delivery and Nanomedicine, Faculty of Pharmacy, Mahidol University, Ratchathewi, Bangkok 10400, Thailand

<sup>c</sup>University of Nottingham, School of Pharmacy, University Park, Nottingham, NG7 2RD, UK

<sup>d</sup>Division of Cancer and Stem Cells, Cancer Biology, University of Nottingham, Nottingham, NG7 2RD, UK

<sup>e</sup>Department of Pharmacology, Faculty of Pharmacy, Mahidol University, Ratchathewi, Bangkok 10400, Thailand

**\*Corresponding author:** Jiraphong Suksiriworapong

Department of Pharmacy, Faculty of Pharmacy, Mahidol University, 447 Sri-Ayudhaya road, Ratchathewi, Bangkok 10400, Thailand

E-mail: [jiraphong.suk@mahidol.ac.th](mailto:jiraphong.suk@mahidol.ac.th)

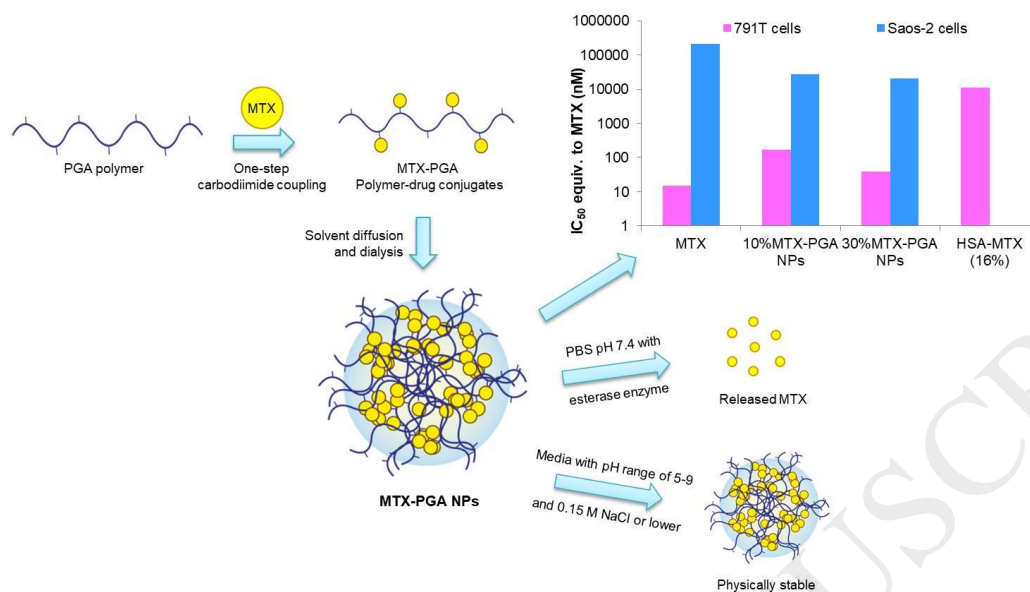
Telephone & Fax: +66-(0)-2644-8694

<sup>1</sup>Present address: School of Life and Medical Sciences, University of Hertfordshire, Hatfield, AL10 9AB, UK

**Total word counts:** 6,048 words (excluding abstract and references)

**Total figures and tables:** 7 (2 tables and 5 figures)

## Graphical abstract



## Highlights

- One step synthesis of MTX-PGA conjugates was succeeded with high molar MTX content.
- The conjugates with ester linker self-assembled to physically stable nanoparticles.
- The MTX release were sustained in buffer pH 7.4 but accelerated by esterase enzyme.
- MTX-PGA NPs had lower potency in 791T but higher toxicity to Saos-2 cells than MTX.
- MTX-PGA NPs showed extremely higher potency in 791T cells than HSA-MTX conjugates.

**Abstract**

Polymer-drug conjugates have been actively developed as potential anticancer drug delivery systems. In this study, we report the first polymer-anticancer drug conjugate with poly(glycerol adipate) (PGA) through the successful conjugation of methotrexate (MTX). MTX-PGA conjugates were controllably and simply fabricated by carbodiimide-mediated coupling reaction with various high molar ratios of MTX. The MTX-PGA conjugate self-assembled into nanoparticles with size dependent on the amount of conjugated MTX and the pH of medium. Change in particle size was attributed to steric hindrance and bulkiness inside the nanoparticle core and dissociation of free functional groups of the drug. The MTX-PGA nanoparticles were physically stable in media with pH range of 5-9 and ionic strength of up to 0.15 M NaCl and further chemically stable against hydrolysis in pH 7.4 medium over 30 days but enzymatically degradable to release unchanged free drug. Although 30%MTX-PGA nanoparticles exhibited only slightly less potency than free MTX in 791T cells in contrast to previously reported human serum albumin-MTX conjugates which had >300 times lower potency than free MTX. However, the MTX nanoparticles showed 10 times higher toxicity to Saos-2 cells than MTX. Together with the enzymic degradation experiments, these results suggest that with a suitable biodegradable polymer a linker moiety is not a necessary component. These easily synthesised PGA drug conjugates lacking a linker moiety could therefore be an effective new pathway for development of polymer drug conjugates.

**Keywords:** Poly(glycerol adipate); Methotrexate; Polymer-drug conjugate; Nanoparticle;

Osteosarcoma cell

**Abbreviations**

HSA-MTX, Human serum albumin-methotrexate conjugates; MTX, Methotrexate; MTX-PGA, Methotrexate-conjugated poly(glycerol adipate); PCE, Porcine carboxylesterase enzyme; PDC, Polymer-drug conjugates; PGA, Poly(glycerol adipate)

## 1. Introduction

Polymer-drug conjugates are once more being actively pursued as potential anticancer agents, and a range of different drugs and polymers are under investigation [1]. Drugs are required to be both potent in molar terms and have a chemical functional group for effective delivery which gives a limited choice, and among the favourites from earlier studies was methotrexate (MTX). There is also a close connection between polymer drug delivery and targeted drug delivery in which drugs are linked to antibodies, and MTX was the first drug to be used for this type of work [2]. The fields of polymer-drug conjugates and antibody targeted MTX are also connected through work by Garnett and co-workers who constructed human serum albumin-MTX (HSA-MTX) conjugates linked to monoclonal antibodies which were particularly potent and selective [3, 4]. This early work on antibody-MTX conjugates has been comprehensively reviewed [5]. MTX still has some advantages in polymer-drug conjugates, as unlike the anthracyclines it is quite robust chemically, but has similar potency in sensitive cancers.

Many efforts have been made to develop macromolecular based drug delivery systems for MTX including polymer-drug conjugates, microparticles and nanoparticles [6, 7]. Several polymers have been proposed to deliver MTX using a polymer-drug conjugate approach such as human serum albumin [8], poloxamer [9], hydroxyethyl starch [10], polypeptide [11], poly(L-lysine) [12], chitosan [13, 14]. Polymer-MTX conjugates can circumvent drug resistance, increase MTX's half-life and potentiate its antitumour efficacy better than the MTX-physically-entrapped particulate carriers [12, 15]. One of the principal causes of MTX resistance is due to

downregulation of uptake pathways, and it has been shown that resistance can be largely overcome by macromolecular conjugates delivered by the lysosomotropic route [16]. A key feature of polymer-drug conjugates is that a biodegradable linkage is required to release drug at the target site through a lysosomotropic mode of action [17, 18]. For many of the earlier conjugates with HSA and poly-L-lysine, it appears to be assumed that these amide-linked natural and semisynthetic polymers would release drug due to the proteolytic degradation in the lysosomal compartment. However, later work by Fitzpatrick and Garnett showed that this degradation was limited and inefficient, and led largely to the release of lysyl-MTX derivatives [19, 20].

In addition to the limited number of drugs which can be conjugated, there are also a limited number of suitable functional polymers for producing polymer-drug conjugates. Key work on understanding polymer-drug conjugates employed hydroxypropyl methacrylamide, a plasma expander [21]. However, as this was a non-biodegradable polymer, suitable linkages to release the drug had to be incorporated and many such linkages have been described [1, 22], but these are mainly designed for drugs like doxorubicin attached by a free amine on the drug. A suitable linkage has also been developed for MTX release [19, 20], however, non-biodegradable polymers have a further disadvantage in that they can be difficult to eliminate from the body. For the production of the simplest and most effective polymer-drug conjugates, a biodegradable functional polymer would be the best way forward, eliminating the need for inclusion of a degradable linker.

Poly(glycerol adipate) (PGA) has been introduced in the pharmaceutical and drug delivery fields due to its versatility and well-suited characteristics for potential clinical use. It consists of two non-toxic monomers, namely glycerol and adipic acid, linked with ester bonds [23]. Major

advantages of PGA are biocompatibility with the body and biodegradability by human enzymes producing non-toxic removable metabolites [24]. Further major advantages over other biodegradable amphiphilic polymers is that every repeating unit of PGA contains a pendant hydroxyl group along the polymer backbone offering the potential for high drug loading using an easy synthetic route. The conjugation of MTX at available hydroxyl groups of PGA leads to a hydrolysable ester linkage of the conjugates which may release the active parent free drug after internalisation in cancer cells. Previously used polymers have significant disadvantages. Albumin and poly-L-lysine do not result in significant release of free drug [8, 12]. Poloxamer, hydroxyethyl starch and chitosan are not significantly biodegradable and polymers such as poloxamer have only terminal groups available for conjugation of drug [9, 10, 13, 14]. These properties variously result in low drug loading and lower cytotoxicity compared to the parent drug. Furthermore, recent work on MTX-conjugated biodegradable poly( $\epsilon$ -caprolactone)-co-poly(ethylene glycol) required several steps of synthesis and inclusion of a triazole linker between drug and polymer [25, 26]. Therefore, the above characteristics of PGA are advantageous and potential for anticancer drug delivery. Up to now, there have been no reports on polymer-anticancer drug conjugates using PGA as a backbone.

The aim of the present work is to synthesise MTX-PGA polymer-drug conjugates and to determine their properties. Due to the amphiphilicity of the polymer [27], the polymer-drug conjugates are expected to be assembled into small nanoparticles in a similar fashion to that reported by the Kataoka group on PEG-polyaspartate-adriamycin conjugate micelles [28]. Also we aim to assess their efficacy for this work in comparison to historical efficacy data on HSA-MTX conjugates to help elucidate mechanistic advantages which may lead to development of more effective polymer-drug conjugates for cancer therapy.

## 2. Materials and methods

### 2.1. Materials

PGA was synthesized according to the previously published method [29]. MTX and porcine carboxylesterase (PCE, with activity of 18 units/mg solid) were used as received from Sigma-Aldrich, Missouri, USA. N,N'-Dicyclohexylcarbodiimide (DCC), 4-(dimethylamino)pyridine (DMAP) were bought from Fluka, Tokyo, Japan. Osteosarcoma cell line 791T originally obtained from the U.S. Naval Biomedical Center, Oakland, USA [30], was obtained from Prof L Durrant, Department of Medicine, Nottingham City Hospital, University of Nottingham, a culture of the cell line used in the works originally published by Garnett et al [3, 4, 19, 20]. Saos-2 cell line (human primary osteogenic sarcoma, ATCC number HTB-85) was kindly gifted from Dr. Pakpoom Kheolamai, Division of Cell Biology, Faculty of Medicine, Thammasat University, Thailand. Eagles Minimum Essential Medium (MEM) and glutamine solution were obtained from Sigma-Aldrich (Dorset, UK). Dulbecco's modified Eagle's medium (DMEM) powder, low glucose, Dulbecco's phosphate buffered saline (DPBS) without calcium chloride without magnesium chloride and PrestoBlue<sup>®</sup> cell viability reagent were purchased from Life Technologies Corporation, Oregon, USA. Sodium pyruvate was obtained from Merck KGaA, Damstadt, Germany. 0.05% Trypsin-EDTA was collected from Gibco<sup>®</sup> (Invitrogen Ltd, Paisley, UK). Resazurin was sourced from Acros Organics (Loughborough, UK). Foetal bovine serum (FBS) was supplied by Invitrogen Ltd (Paisley, UK). Commercially available sterile methotrexate solution for injection (25 mg/mL) was obtained from Mylan, Hatfield, UK. Dimethyl formamide (DMF) and acetonitrile were of high performance liquid chromatography (HPLC) grade and used as received. Dimethyl sulfoxide (DMSO) was dried using molecular sieves prior to use. Water employed throughout this study was deionized (DI) grade or higher.

## **2.2. Synthesis of MTX-conjugated PGA (MTX-PGA) polymers**

Conjugates of varying nominal MTX % mole with respect to PGA polymer repeating unit were produced by a simple carbodiimide coupling reaction. In brief, PGA (1 g = 4.95 mmole glycerol adipate repeating units) was dissolved in dried DMSO (10 mL). Calculated amounts of MTX (1.5 equiv.), DCC (1.2 equiv.) and DMAP (0.3 equiv.) relative to the mol% nominal value of polymer repeating units were then added. The reaction was stirred for 72 h and protected from light. After that, the precipitate was removed by centrifugation at 4500 rpm, 4°C for 15 min. The supernatant was collected and precipitated in methanol. The precipitate was washed with methanol for another 3 times and re-dissolved in a small volume of DMSO. The polymer solution was dialyzed against DI water for 24 h using dialysis bag (MWCO 12,400 Da, Sigma-Aldrich, Missouri, USA). Finally, the polymer was freeze dried for 24 h. The dried polymer was kept in a desiccator until use.

## **2.3. Polymer characterization**

### **2.3.1. IR spectroscopy**

Presence of drug in conjugated PGA polymer was first assessed by infrared (IR) spectroscopy using an Attenuated Total Reflection (ATR) spectrometer (Agilent Cary 630 FTIR, Agilent Technologies, Santa Clara, USA). The spectra were recorded with a resolution of 4 cm<sup>-1</sup> over the range of 4000-650 cm<sup>-1</sup> by recording 32 interferograms.

### **2.3.2. Nuclear magnetic resonance (NMR) spectroscopy**

The quantitation of drug coupling and structure of MTX-PGA polymers were investigated by proton <sup>1</sup>H NMR spectroscopy. The spectra were recorded by Bruker 400 MHz spectrometer (Bruker corporation, Rheinstetten, Germany) using DMSO-*d*<sub>6</sub> as a solvent.

MTX-PGA (DMSO- $d_6$ ;  $\delta$ , ppm): 8.58 (s, 1H), 7.72-7.74 (m, 2H), 6.82-6.84 (d, 2H), 5.26-5.19 (m, 2H), 4.95 (m, 1H), 4.79 (s, 2H), 4.37 (t, 1H), 4.23 (m, 2H), 4.18-3.88 (m, 6H), 3.63 (m, 2H), 3.21 (s, 3H), 2.32 (m, 4H), 2.09 (m, 2H), 1.96 (m, 2H), 1.53 (m, 4H).

PGA (DMSO- $d_6$ ;  $\delta$ , ppm): 5.26-5.19 (m, 2H), 4.95 (m, 1H), 4.27-4.24 (m, 2H), 4.18-3.88 (m, 6H), 3.63 (m, 2H), 2.32 (m, 4H), 1.53 (m, 4H).

### 2.3.3. Gel permeation chromatography (GPC)

The molecular weights (number- and weight-average,  $M_n$  and  $M_w$ , respectively) were measured by gel permeation chromatography (PL50 Plus Polymer Laboratories system) equipped with a refractive index detector. Two mixed PL-Gel 5  $\mu$ m bed (D) columns maintained at 50°C were used as a stationary phase using DMF containing 0.1% LiBr at a flow rate of 1 mL/min as an eluent. Poly (methyl methacrylate) standards ( $M_n$  range of 1,810,000-505 g/mol) were employed to construct a calibration curve.

### 2.3.4. UV analysis of MTX content

The amount of conjugated MTX was analysed by UV/Vis spectrophotometer (UV-2600, Shimadzu Corporation, Kyoto, Japan). The absorbance value of the polymers was measured in DMF at a wavelength of 412 nm. The amount of conjugated MTX was calculated from a calibration curve of MTX over the range of 5-100  $\mu$ g/mL. The molar absorptivity of MTX in DMF was  $3.6643 \times 10^3 \text{ M}^{-1}$ .

## 2.4. Nanoparticle formation

The nanoparticles of MTX-PGA polymers (MTX-PGA NPs) were prepared by a solvent diffusion and dialysis method [26]. In brief, 10 mg of the polymer was dissolved in 1 mL of DMSO. This solution was then added dropwise to 1 mL of aqueous phase while stirring to allow solvent diffusion. Then the colloidal dispersion was sealed in a dialysis tube (MWCO 1 kDa,

Spectra/Por<sup>®</sup> 6, Spectrum Laboratories, Inc., Dominguez, USA) for 24 h. The assembled nanoparticles were collected and kept as a dispersion until use.

### ***2.5. Analyses of particle size, size distribution and zeta potential***

The mean hydrodynamic diameter (z-ave), size distribution (PDI) and zeta potential (ZP) were assessed by Zetasizer NanoZS (Malvern Instrument Ltd., Malvern, UK). The sample without dilution was measured with He-Ne laser at a wavelength of 633 nm, an angle of 173° and 25°C. The ZP of nanoparticles was evaluated according to the electrophoretic mobility of the particles and calculated by the Helmholtz-Smoluchowsky equation. All measurements were performed in triplicate.

### ***2.6. Physical stability of nanoparticles in various pHs and ionic strengths***

To evaluate effects of pH and ionic strength of medium on the stability of the nanoparticles, the nanoparticles were diluted 10-fold in water adjusted to various pHs (1-13) using 5 M HCl or NaOH and to different ionic strengths (0.05-0.50 M sodium chloride solution; NaCl) using 5 M NaCl solution, respectively [31]. After mixing for 5 min, the sample was examined for hydrodynamic diameter, PDI and derived count rate. The derived count rate reflecting aggregation, sedimentation or dissociation of the nanoparticles is illustrated as kilo counts per second (kcps). The results are expressed as relative values of hydrodynamic diameter, PDI or kcps in the changed medium compared to an equal dilution of the nanoparticles in sterile water for injection.

### ***2.7. In vitro non-enzymatic and enzymatic drug release studies***

The drug release study of MTX-PGA NPs was performed in 25 mM phosphate buffered saline (PBS) pH 7.4 by dialysis method [26]. A typical protocol for release study was as follows. Freshly prepared MTX-PGA NPs (1 mL) were measured into a dialysis bag (MWCO 1000 Da,

Spectra/Por 6, Spectrum Laboratories, Inc., Dominguez, USA). The tightly sealed bag was immersed in the external medium (20 mL PBS pH 7.4 containing 0.02% w/v sodium azide). The release study was conducted at 37°C in the light-protected container with magnetic stirring at 100 rpm. At predetermined times, sample (1 mL) was withdrawn from the external medium and was replenished with an equal volume of fresh PBS. In the case of enzymatic drug release study, porcine carboxylesterase (PCE) enzyme was mixed with the nanoparticle dispersion yielding 20 and 50 units/mL of PCE [32-34]. The NPs mixture was filled into the dialysis bag and the release study was similarly performed as previously described. The enzymatic release study was conducted for 7 days. The MTX solution was employed as a control. The amount of MTX in the sample was analysed by HPLC (Shimadzu HPLC apparatus, Shimadzu Corporation, Kyoto, Japan) using Luna C18 column 150×4.6 mm plus a C18 guard column (Phenomenex, Torrance, USA) as a stationary phase and the mixture of 10% v/v acetonitrile and 90% v/v 0.05 M phosphate buffer pH 6.0 at a flow rate of 1.2 mL/min as a mobile phase.

## ***2.8. Cytotoxicity test in 791T osteosarcoma cells***

### ***2.8.1. Cell culture experiment***

The osteosarcoma cell line 791T was grown as a monolayer in tissue culture polystyrene flasks in Eagles Minimum Essential Medium with the addition of 10% foetal bovine serum and 20 mM glutamine. Medium was changed every 2-3 days and cells were detached using 0.05% trypsin-EDTA for subculture. The cells were kept in an incubator at 37°C with a humidified atmosphere with 5% CO<sub>2</sub>.

### ***2.8.2. Drug solution and nanoparticle suspension preparation***

Commercially available sterile MTX solution for injection (25 mg/mL, 55 mM in saline), and sterile-filtered nanoparticle suspensions (115-173 µM MTX equivalent) in PBS were diluted in

cell-culture medium to 9 half- $\log_{10}$ -spaced concentrations spanning from (2 nM to 200  $\mu$ M). MTX concentrations for the nanoparticle suspensions were calculated from UV absorption measurements. Drugs and nanoparticles were added as 2 $\times$  solutions (100  $\mu$ L/well) to build a dose-response from 1 nM to 100  $\mu$ M. PBS concentration in all wells was kept at 10% v/v. For incubations longer than 72 h, media was refreshed with solutions/suspensions with the nominal MTX concentration equivalent. There were 6 technical replicates for each condition.

### *2.8.3. Drug treatment in monolayer*

791T cells were seeded in flat bottom cell culture treated 96-well plates (100  $\mu$ L,  $20 \times 10^3$  cells/mL) and left in the incubator for 24 h. Drug solution and nanoparticle suspensions were added from 2 $\times$  stocks and left for 72 h. For the 6-day treatment experiments in monolayer, the old medium (150  $\mu$ L) was removed, replaced with fresh drug solution (150  $\mu$ L) and the cells cultured for another 72 h. On days 4 and 7 cell viability was determined using the resazurin assay.

### *2.8.4. Drug treatment for spheroid cultures*

791T cells were seeded in round bottom ultra-low attachment 96-well plates (100  $\mu$ L,  $10 \times 10^3$  cells/mL) and left to incubate for 72 h. MTX and MTX-PGA NPs were added on day 3 from 2 $\times$  stock solutions, then refreshed on day 6. Spheroids were imaged on days 3, 6, and 9 and resazurin activity was determined on days 6 and 9.

### *2.8.5. Resazurin assay*

Assay-ready resazurin solution (60  $\mu$ M) was prepared from resazurin stock solution (440  $\mu$ M in Hank's Buffered Salt Solution) and fresh cell culture media. Spent medium (150  $\mu$ L) was removed from each well and replaced with the same volume of assay resazurin solution. Cells in monolayer were incubated for 2 h, while spheroids were left for 4 h in the incubator.

Fluorescence was measured with an excitation wavelength of 530 nm and emission 590 nm on a Flexstation II plate reader.

#### *2.8.6. Spheroid imaging*

Brightfield spheroid images were acquired with a Nikon Ti Eclipse inverted microscope using 4 × objective. Spheroid volume was determined with an in-house open source macro for the FiJi distribution of ImageJ [35, 36].

### **2.9. Cytotoxicity test in Saos-2 osteosarcoma cells**

#### *2.9.1. Cell culture experiment*

Saos-2 cells were cultured in Dulbecco's modified Eagle's medium (DMEM) supplemented with 10% FBS and penicillin/streptomycin (100 units/mL) in a 5% CO<sub>2</sub> humidified incubator at 37°C. The medium was change every 2-3 days. For subculture, the cells were trypsinised using 0.25% trypsin-EDTA.

#### *2.9.2. Drug solution and nanoparticle suspension preparation*

MTX stock solution was prepared in Dulbecco's PBS pH 7.4. The stock solutions of MTX and nanoparticles were filtered through sterile 0.22 µm syringe filter and subsequently diluted in DMEM to the concentration range of 0.002 – 220 µM.

#### *2.9.3. Drug treatment in Saos-2 monolayer*

Saos-2 cells (100 µL) were seeded in 96-well plate at a cell density of 2,000 cells/well and incubated under 5% CO<sub>2</sub> humidified atmosphere at 37°C for 24 h. After aspirating the medium, 100 µL of sample was subsequently added into each well and the cells were incubated for 72 h. After that PrestoBlue<sup>®</sup> cell viability reagent (10 µL) was added in each well and then incubated for 50 min in the incubator. The absorbance was measured at 570 and 600 nm as measuring and reference wavelengths, respectively, by a microplate reader (Tecan's Infinite<sup>®</sup> 200 NanoQuant,

Männedorf, Switzerland). The measurement was performed in six replicates for at least 2 different days.

### **2.10. Statistical analysis**

The z-ave, PDI and ZP of MTX-PGA NPs were statistically compared using one-way ANOVA (IBM SPSS statistic 21). The significant difference is considered when  $p$ -value is less than 0.05. Data from resazurin experiments were normalized to untreated controls (100% viability) and cell-free wells (0% viability). The volume of untreated spheroids was taken as 100% viability and 0 as 0% viability. Four-parameter logistic dose-response curves were fitted to the resazurin, volume and PrestoBlue® data in GraphPad Prism, the top was constrained to 100 and the bottom to  $\geq 0$ . IC<sub>50</sub>s used are the inflection point of the dose-response curve, half-way between the untreated controls (100%) and the curve bottom (maximum effect). Results are displayed as mean  $\pm$  SD unless stated otherwise.

## **3. Results and Discussion**

### **3.1. Conjugation of MTX onto PGA backbone**

By a simple coupling reaction, various amounts of MTX were successfully conjugated to the PGA backbone, which were designated X%MTX-PGA, with X corresponding to the nominal mole% MTX per polymer repeating unit. As compared to the IR-ATR spectrum of PGA (Fig. 1A), the sharp C=O stretching peak at 1718 cm<sup>-1</sup> corresponding to the ester coupling of MTX and glycerol adipate repeating unit overlapped to that ester along the PGA backbone. Other characteristics of MTX were also observed in the spectra. The peaks of N-H bending of amine, C=O stretching of amide bond, C=C stretching of aromatic ring of MTX were overlapping to each other at 1624, 1600 and 1553 cm<sup>-1</sup>, respectively. However, the intensity of these peaks increased with the MTX content. The peaks of N-H stretching of amine and amide occurred over

the region of 2950-2800  $\text{cm}^{-1}$  which overlapped with O-H stretching of PGA. As previously reported on the NMR spectrum of PGA, the adipic protons presented at 1.5 and 2.3 ppm in  $\text{DMSO-}d_6$  (Fig. 1B) which slightly shifted to upfield region as compared to those in  $\text{acetone-}d_6$  [29]. Meanwhile, the protons related to glycerol repeating units were apparent in the region of 3.6 ppm and 4.9 ppm. The methine protons corresponding to 1,2 and 1,3 di-substituted glycerides occurred at 5.20 ppm coinciding with the presence of the methine proton of 1,2,3 tri-substituted glycerol units at 5.26 ppm. The latter proton indicates the tri-substituted repetitive glycerol unit of PGA polymer. The conjugation of MTX at free hydroxyl group available on glycerol units resulted in the shift of methylene proton peaks from 3.6 ppm to 4.2 ppm. The methine proton at 5.26 ppm increased when higher amounts of MTX were conjugated, confirming the functionalization of the secondary hydroxyl group. The glycerol and adipic protons of MTX-PGA polymers were still observed at a similar chemical shift to those of PGA. In addition, the characteristic protons of MTX were also observed in the NMR spectra.

**Fig. 1**

The percent MTX conjugation can be calculated from NMR spectra based on the pteridine proton of MTX at 8.58 ppm and the methylene protons in adipate units of PGA at 2.32 ppm as shown in the equation (1). The methine proton at 5.26 ppm could not be accounted for in the calculation of % conjugated MTX due to the interference of methine proton of di-substituted repeating units. The results are illustrated in Table 1. The % conjugated MTX was found to be 7.0, 14.5 and 27.5% with respect to number of repeating units of PGA chain for 10%, 20% and 30% MTX-PGA, respectively. Using these NMR data, the conjugation efficiency based on theoretical conjugation reached 58.3, 60.4 and 76.4% for 10%, 20% and 30% MTX-PGA, respectively. The amount of conjugated MTX was further confirmed by UV spectrophotometry.

The analysed amount of MTX was found to be  $8.86 \pm 0.32$ ,  $17.33 \pm 1.25$ ,  $33.26 \pm 4.72$  %mole MTX conjugated per mole of polymer repeating unit. The difference between the analysis using NMR and UV spectrophotometry is probably due to changes in extinction coefficients on conjugation of MTX.

$$\frac{I_{8.58 \text{ ppm}/1}}{I_{2.32 \text{ ppm}/4}} \times 100 \quad (1)$$

where  $I_{8.58 \text{ ppm}}$  and  $I_{2.32 \text{ ppm}}$  are the integrals of pteridine proton of MTX at 8.58 ppm and methylene protons in adipate repeating units of PGA at 2.32 ppm, respectively.

### Table 1

The  $M_n$  of PGA starting materials was 13000 g/mol. After conjugation, the  $M_n$  of MTX-PGA polymers increased gradually with %MTX conjugation. The  $M_w/M_n$  values of all MTX-PGA polymers decreased compared to that of PGA due to the purification of polymer by precipitation in which the unconjugated PGA could be removed during washing which may tend to selectively remove the lower molecular weight polymers. These results indicated that MTX was successfully conjugated along PGA backbone by a simple carbodiimide-mediated coupling reaction.

### 3.2. Nanoparticle formation

The MTX-PGA NPs were prepared in deionized water by solvent diffusion-dialysis method. As shown in Fig. 2, the hydrodynamic diameter of MTX-PGA NPs tended to increase with %MTX except for 20%MTX-PGA nanoparticles whose value was extraordinarily larger than the others. The particle size of 20% and 30%MTX-PGA was approximately 6 and 2 times larger than 10%MTX-PGA NPs, respectively. The increasing particle size with drug loading may be due to higher steric hindrance and bulkiness inside the nanoparticle core as a result of poor packing of drug moiety as seen in the case of 20%MTX-PGA NPs. Meanwhile, for 30%MTX, a better

compaction of the nanoparticles was achieved, probably due to increased hydrophobicity of the polymer-drug conjugates. The size distribution of 10% and 30%MTX-PGA NPs was narrow while, that of 20%MTX-PGA NPs was quite broad. The size distribution related to the diameter of the nanoparticles. A greater negative surface charge of nanoparticles was observed when increasing %MTX in particular to 30%MTX-PGA NPs indicating that an increasing number of MTX moieties was displayed on the nanoparticle surface. Combining the results of hydrodynamic diameter and zeta potential, the dramatic size increase of 20%MTX-PGA NPs was thought to result from destabilization of the nanoparticles followed by agglomeration upon particle formation.

**Fig. 2**

From these results, we anticipated that the pH of preparation medium may affect the particle formation due to a presence of pH-sensitive moiety in the drug molecule. Therefore, the effect of pH of preparation medium was further investigated. Two pH media were used, namely acidic pH 3.0 medium and pH 7.4 medium. As expected, the pH of preparation medium considerably affected the hydrodynamic diameter. In medium pH 7.4, the particle size decreased with increasing %MTX. Meanwhile, the diameter of nanoparticles gradually increased in acidic pH 3.0 medium with increasing %MTX. This result was likely caused by the acid dissociation of MTX in different medium pHs. MTX possesses three pKa value ranges of 3.3-3.4, 3.9-4.7 and 5.3-5.7 at alpha and gamma carboxyl groups and pteridine ring, respectively [37, 38]. The gamma carboxyl of MTX is more reactive so tend to conjugate to hydroxyl pendant of PGA more readily resulting in a higher preponderance of free alpha carboxyl group [39], so the free carboxyl and pteridine of MTX are involved in the dissociation of MTX in the medium. MTX protons were almost totally dissociated in medium pH 7.4 [40] while acid groups remained

unionized at pH 3.0. The ionized MTX molecule exhibited more hydrophilicity and favoured an aqueous phase. Thus the drug molecules were preferably presented on the surface of particles and fewer molecules incorporated in the core thus dramatically reducing the particle size to less than 100 nm. On the other hand, the acidic aqueous phase suppressed the dissociation of carboxylic group of MTX which enhanced the hydrophobicity of drug molecules and nanoparticle core. Thus, it enlarged the MTX-PGA NPs with increasing MTX content. The size distribution of the nanoparticles increased in acidic medium but declined in pH 7.4 medium relative to that in deionized water. The zeta potential of MTX-PGA NPs became positive and more negative in media pH 3.0 and 7.4, respectively. The difference in amount of MTX did not affect the zeta potential ( $p$ -value>0.05). The change of surface charge of MTX-PGA NPs was possibly as a result of ionised hydronium and hydroxyl species in the acidic and pH 7.4 media, respectively.

### ***3.3. Physical stability of nanoparticles in various pHs and ionic strengths***

The physical stability of MTX-PGA NP dispersion was evaluated in various pHs and ionic strengths. The relative hydrodynamic diameter, PDI and kcps compared to the nanoparticles equally diluted in sterile water for injection are summarised in Fig. 3. Regarding the effect of pH, the hydrodynamic diameter of all MTX-PGA NPs increased by at least twice in extremely low and high pHs (1-3 and 11-13). The size distribution was also broadened particularly to 10%MTX-PGA NPs over pH range of 1-3 and 11-13. The relative kcps of MTX-PGA NPs in pH 1-3 considerably increased especially 20%MTX-PGA NPs whilst it decreased in pH 11-13. Principally, an increase of count rate suggests an occurrence of aggregation of particles whereas a decrease of count rate indicates the sedimentation or dissociation of nanoparticles [41, 42].

Combining the hydrodynamic diameter and *z*-pots data, the MTX-PGA NPs aggregated into large particles in media with pH of less than 5 and dissociated or settled down in media pH over 7.

### **Fig. 3**

Regarding the effect of ionic strength, the nanoparticles started to aggregate in 0.25 M NaCl as seen by dramatic increases of hydrodynamic diameter and PDI. Meanwhile, the increment of *z*-pots was initially observed in 0.15 M NaCl particular to 20%MTX-PGA NPs whereas the others remained almost unchanged. The results indicated that all MTX-PGA NPs aggregated in the medium with NaCl concentration of 0.25 M or higher. 10%MTX-PGA NPs and 30%MTX-PGA NPs were physically stable in the medium with 0.15 M NaCl or lower. From the results above, it was suggested that the MTX-PGA NPs were physically stable in physiological relevant medium with pH range of 5-9 and ionic strength of lower than 0.15 M NaCl.

### **3.4. *In vitro* drug release experiment**

We have chosen carboxylesterase (PCE) as an example of an enzyme which can degrade PGA to investigate drug release. The hydrolytic release of MTX from MTX-PGA NPs was investigated in PBS pH 7.4 over 30 days. The results are graphically demonstrated in Fig. 4. The control MTX solution showed a rapid diffusion from the dialysis tubing with over 90% release within 8 h. Meanwhile, the MTX release from all MTX-PGA NPs was considerably slower over 30 days showing effective conjugation of the drug to the polymer with only a slow hydrolytic degradation. The maximum MTX release provided by 30%MTX-PGA NPs reached only 17% at day 30. Regarding various %MTX conjugations, the extent of MTX release depended on the amount of conjugated MTX. 10%MTX-PGA NPs released the lowest amount of MTX by only 9% at the end of experiment even though they had smallest average diameter after preparation. The presence of esterase enzyme in PBS accelerated the release of MTX from 30%MTX-PGA

NPs. Moreover, the rate of MTX release escalated with the PCE concentration. At day 7, 40% and 62% of MTX were released in PBS containing 20 and 50 units/mL PCE, respectively. The liberated MTX peak in HPLC chromatogram was identical to the MTX standard peak (data not shown) suggesting that the degradation of MTX-PGA NPs could be catalysed by esterase enzyme liberating intact MTX molecules whose pharmacological activity should not be changed. There are a wide range of proteolytic enzymes present in the lysosomal environment with different specificities and this can be illustrated with a previous paper by our group which reported the uptake and metabolism of PGA nanoparticles in DAOY cells [43]. The PGA nanoparticles are taken up by the cells which then enter endosomes and lysosomes and undergo fast degradation in the cells. This environment is likely to result in a much faster and complete degradation and drug release than seen in the present experiment. However the above experiment demonstrates the potential for an enzymic release of free drug from this polymer which is more effective than the release of MTX previously reported from HSA-MTX conjugates using lysosomal enzyme preparations [19, 20].

#### **Fig. 4**

#### ***3.5. Cell response experiment***

To further confirm the potency of MTX-PGA NPs, a cell response experiment was performed in osteosarcoma 791T cells. 10%MTX-PGA NPs and 30%MTX-PGA NPs were selected to study their cell response in comparison with the clinically available MTX solution. MTX and MTX-PGA NPs elicited a dose dependent decrease in 791T cell viability after incubation for 72 h (Fig. 5). The cytotoxic effects of MTX and the nanoparticles were more pronounced in monolayer cultures (Fig. 5A), where MTX had an  $IC_{50}$  of 15 nM and killed 75% of cells. These results are

in agreement with previous studies on the cytotoxic effects of MTX in monolayer by Garnett et al [4].

### **Fig. 5**

Present results of MTX-PGA NPs and historic results with HSA-MTX by Garnett et al. (Fig. S1 in supplementary data) are compared using 791T cells in 2D cell culture. Values in parenthesis give % drug loading w/w as drug loading appears to affect cytotoxicity. The MTX-PGA analogues were 2.6 and 11.3 times less potent compared to free MTX. This is significantly better compared to the >300× potency differences seen with the HSA-MTX conjugates (Table 2). The increased potency of the MTX-PGA analogues compared to HSA-MTX is probably due to the quick degradation of PGA in the lysosomes once internalized in the cells. MTX-PGA NPs were probably degraded to free drug by enzyme-catalysed hydrolysis as seen in the enzymatic release experiment. This is in contrast to HSA-MTX conjugates which mainly released the lysyl-MTX derivatives [19, 20]. It has been reported that the efficiency of dihydrofolate reductase inhibition of MTX is lowered by conjugation due to steric interference between the enzyme and the modified drug [44, 45]. Therefore, the higher potency of MTX-PGA NPs as compared to HSA-MTX may be attributed to improved free drug release.

### **Table 2**

It has been demonstrated in previous publications by our group that there is a greater uptake of PGA nanoparticles into DAOY tumour spheroids than for similar mixed rat neonatal normal brain cells [46], and we have recently published a convenient method for determination of cytotoxicity in spheroid cultures [35]. We have therefore also investigated the cytotoxicity of MTX-PGA NPs in 791T spheroids compared to free drug. The results for resazurin reduction in 791T spheroids were considerably more variable compared to monolayers resulting in

ambiguous curve-fits (Fig. 5B). Nevertheless, a similar trend was observed, where free MTX was the most potent, closely followed by 30%MTX-PGA (1.2 times  $IC_{50}$  difference) and 10%MTX-PGA was the least potent (30 times  $IC_{50}$  difference). When spheroid volume was used to estimate spheroid viability, variability was much lower, curve fitting and the estimation of  $IC_{50}$ s and maximal effects improved (Fig. 5C). Although MTX was still active in the nanomolar range ( $IC_{50}=45$  nM), cell viability remained above 50% even at micromolar concentrations. Increased resistance to chemotherapy when cells are cultured in 3D has been reported before [35, 47, 48]. Notwithstanding the decrease in sensitivity, the potency differences between MTX and the MTX-PGA conjugates remained unchanged (Fig. 5D). Longer incubation periods (6 days) produced even more potent responses to MTX with lower  $IC_{50}$ s and smaller surviving fraction of cells, along with similar potency ratio between the free drug and the conjugates (Fig. S2 in supplementary data). It was disappointing that the 3D culture conditions did not show an improvement in relative activity of MTX-PGA/MTX compared to 2D culture but this may be due to other factors like the physicochemical properties of the nanoparticles and their cellular interactions.

Further investigation was performed in another osteosarcoma cell line, Saos-2, to further confirm whether the MTX-PGA NPs would affect in a similar or different fashion as observed in 791T cells. The  $IC_{50}$  values of MTX-PGA NPs against Saos-2 cells are summarised in Table 2. MTX had an  $IC_{50}$  of 210.9  $\mu$ M in Saos-2 and only resulted in 47.7% cell viability even at the highest concentration of MTX tested in this study. This value was high in the micromolar range and extremely high compared to the value in 791T cells but was consistent with previous studies on low MTX-responsive or MTX-resistant Saos-2 cells [49, 50]. In the case of MTX-PGA NPs, 10%MTX-PGA NPs and 30%MTX-PGA NPs were relatively unresponsive on Saos-2 in

comparison to 791T cells with  $IC_{50}$ s of 26.8 and 20.2  $\mu$ M, respectively. Although the  $IC_{50}$  values of the nanoparticles on Saos-2 cells were still in the micromolar range, they possessed 7.9 and 10.4 times higher potency than free drug, respectively. This result revealed that the MTX-PGA NPs provided better relative potency in Saos-2 cells than 791T cells suggesting the improved efficacy of MTX-PGA conjugates in Saos-2 cells. As evidenced by the previous reports [49, 50], the low MTX-responsive or MTX-resistant Saos-2 cells are attributed to a reduction of MTX uptake by RFC, an overexpression of DHFR protein, an increment of MTX efflux due to overexpression of multidrug resistant protein, a reduction of MTX polyglutamylation, a decrease of DHFR affinity to MTX and the combination of these mechanisms [50-52]. The improved efficacy in Saos-2 cells by the MTX-PGA NPs may be attributed to overcoming one of the resistance mechanisms. Further work will be needed to investigate the mechanistic resistance of Saos-2 to MTX and to evaluate whether the MTX-PGA NPs can be used in MTX-resistant osteosarcoma.

## 5. Conclusion

Our study showed the feasibility of the conjugation of anticancer drug, MTX, to a PGA backbone, the first polymer-anticancer drug conjugate reported with this polymer. The MTX-PGA conjugates contained high molar MTX content by 27.5 mole% and showed promising characteristics in terms of particle properties, physical stability in the physiological medium, stability of polymer-drug conjugate linker over 30 days and enzymatic degradability. Although the MTX-PGA NPs showed lower cytotoxicity to 791T cells than free MTX, 30% MTX-PGA NPs were only slightly less potent than MTX in either 2D or 3D cultures. Nonetheless, the nanoparticles exhibited relatively higher toxicity to Saos-2 cells than the parent drug. The improved efficacy of MTX in Saos-2 cells rather than 791T cells was possibly due to

surmounting MTX-resistant mechanism in this cell. However, further work is needed to determine the mechanism overcoming the drug resistance by MTX-PGA NPs. Taking the enzymic degradation results together with the cytotoxicity data and previous reports on the degradation of PGA in the lysosomal compartment of cells, this strongly suggests that this PGA polymer conjugate does not require a complex linker between drug and polymer. This opens the way to a possible new paradigm for polymer-drug conjugates which have a simpler synthesis together with a more effective mechanism of action. Nevertheless, further improvement of potency and greater specificity of the conjugate may be needed for this type of polymer-drug conjugate and we are continuing to investigate these possible improvements.

### **Acknowledgements**

This work was financially supported by the Thailand Research Fund, the Office of the Higher Education Commission (Thailand) and Mahidol University (Thailand) through Research Grant for New Scholar [grant number MRG5980026]. Authors also thank the support from British Council Newton Fund through the Researcher Links Travel Grants for initiating our collaboration. Dr. Pakpoom Kheolamai, Division of Cell Biology, Faculty of Medicine, Thammasat University, Thailand, is also acknowledged for providing Saos-2 cells used in this study. Vincenzo Taresco was supported by Engineering and Physical Sciences Research Council (EPSRC) [grant number EP/L013835/1], Delyan Ivanov by the EPSRC Doctoral Training Prize scheme hosted by the University of Nottingham [grant number EP/M506588/1] and Ioanna Styliari by the EPSRC CDT in Targeted Therapeutics [grant number EP/I01375X/1].

### **Conflict of Interest**

The authors declare no competing financial interest.

**References**

1. Q. Feng and R. Tong, *Bioeng Transl Med*, 1(3) (2016) 277.
2. G. Mathé, Tran Ba Loc and J. Bernard, *C R Acad Sci (Paris)*, 246 (1958) 1626.
3. M. C. Garnett and R. W. Baldwin, *Cancer Res*, 46(5) (1986) 2407.
4. M. C. Garnett, M. J. Embleton, E. Jacobs and R. W. Baldwin, *Int J Cancer*, 31(5) (1983) 661.
5. M. C. Garnett, *Adv Drug Deliv Rev*, 53(2) (2001) 171.
6. J. Chen, L. Huang, H. Lai, C. Lu, M. Fang, Q. Zhang and X. Luo, *Mol Pharm*, 11(7) (2014) 2213.
7. H. Kang, J. D. Kim, S. H. Han and I. S. Chang, *J Controlled Release*, 81(1–2) (2002) 135.
8. B. C. Chu and J. M. Whiteley, *Mol Pharmacol*, 13(1) (1977) 80.
9. Y. Chen, W. Zhang, Y. Huang, F. Gao, X. Sha, K. Lou and X. Fang, *Int J Nanomed*, 10 (2015) 4043.
10. T. M. Goszczyński, B. Filip-Psurska, K. Kempieńska, J. Wietrzyk and J. Boratyński, *Pharmacol Res Perspect*, 2(3) (2014) e00047.
11. G. Kóczán, A. C. Ghose, A. Mookerjee and F. Hudecz, *Bioconj Chem*, 13(3) (2002) 518.
12. H. J.-P. Ryser and W.-C. Shen, *Proc Natl Acad Sci USA*, 75(8) (1978) 3867.
13. Y. Wang, X. Yang, J. Yang, Y. Wang, R. Chen, J. Wu, Y. Liu and N. Zhang, *Carbohydr Polym*, 86(4) (2011) 1665.
14. D.-H. Seo, Y.-I. Jeong, D.-G. Kim, M.-J. Jang, M.-K. Jang and J.-W. Nah, *Colloids Surf B Biointerfaces*, 69(2) (2009) 157.

15. C.-K. Kim and S. J. Hwang, *Drug Dev Ind Pharm*, 19(8) (1993) 961.
16. K. Affleck and M. J. Embleton, *Br J Cancer*, 65(6) (1992) 838.
17. C. De Duve, T. De Barsey, B. Poole, A. Trouet, P. Tulkens and F. Van Hoof, *Biochem Pharmacol*, 23(18) (1974) 2495.
18. H. Ringsdorf, *J Polym Sci, Part C: Polym Symp*, 51(1) (1975) 135.
19. J. J. Fitzpatrick and M. C. Garnett, *Anticancer Drug Des*, 10(1) (1995) 11.
20. J. J. Fitzpatrick and M. C. Garnett, *Anticancer Drug Des*, 10(1) (1995) 1.
21. J. Kopeček and H. Bažilová, *Eur Polym J*, 9(1) (1973) 7.
22. J. Khandare and T. Minko, *Prog Polym Sci*, 31(4) (2006) 359.
23. P. Kallinteri, S. Higgins, G. A. Hutcheon, C. B. St. Pourçain and M. C. Garnett, *Biomacromolecules*, 6(4) (2005) 1885.
24. V. Taresco, J. Suksiriworapong, I. D. Styliari, R. H. Argent, S. E. Swainson, J. Booth, E. Turpin, C. A. Laughton, J. C. Burley, C. Alexander and M. C. Garnett, *RSC Adv*, 6(111) (2016) 109401.
25. O. Issarachot, J. Suksiriworapong, K. Sripha and V. B. Junyaprasert, *J Appl Polym Sci*, 129(2) (2013) 721.
26. O. Issarachot, J. Suksiriworapong, M. Takano, R. Yumoto and V. B. Junyaprasert, *J Nanopart Res*, 16(2) (2014) 2276.
27. V. Taresco, R. G. Creasey, J. Kennon, G. Mantovani, C. Alexander, J. C. Burley and M. C. Garnett, *Polymer*, 89 (2016) 41.
28. M. Yokoyama, T. Sugiyama, T. Okano, Y. Sakurai, M. Naito and K. Kataoka, *Pharm Res*, 10(6) (1993) 895.

29. V. Taresco, J. Suksiriworapong, R. Creasey, J. C. Burley, G. Mantovani, C. Alexander, K. Treacher, J. Booth and M. C. Garnett, *J Polym Sci, Part A: Polym Chem*, 54(20) (2016) 3267.
30. M. J. Embleton, B. Gunn, V. S. Byers and R. W. Baldwin, *Br J Cancer*, 43(5) (1981) 582.
31. P. Charoongchit, J. Suksiriworapong, K. Sripha, S. Mao, A. Sapin-Minet, P. Maincent and V. B. Junyaprasert, *Mater Sci Eng, C*, 72 (2017) 444.
32. S. Samarajeewa, A. Ibricevic, S. P. Gunsten, R. Shrestha, M. Elsbahy, S. L. Brody and K. L. Wooley, *Biomacromolecules*, 14(4) (2013) 1018.
33. S.-L. Liang, X.-Y. Yang, X.-Y. Fang, W. D. Cook, G. A. Thouas and Q.-Z. Chen, *Biomaterials*, 32(33) (2011) 8486.
34. T. Siegemund, B. R. Paulke, H. Schmiedel, N. Bordag, A. Hoffmann, T. Harkany, H. Tanila, J. Kacza and W. Hartig, *Int J Dev Neurosci*, 24(2-3) (2006) 195.
35. D. P. Ivanov, T. L. Parker, D. A. Walker, C. Alexander, M. B. Ashford, P. R. Gellert and M. C. Garnett, *PLoS One*, 9(8) (2014) e103817.
36. D. P. Ivanov, A. M. Grabowska and M. C. Garnett, *Methods Mol Biol*, 1601 (2017) 43.
37. M. Shalaeva, J. Kenseth, F. Lombardo and A. Bastin, *J Pharm Sci*, 97(7) (2008) 2581.
38. M. Poe, *J Biol Chem*, 252(11) (1977) 3724.
39. A. Gabizon, A. T. Horowitz, D. Goren, D. Tzemach, F. Mandelbaum-Shavit, M. M. Qazen and S. Zalipsky, *Bioconj Chem*, 10(2) (1999) 289.
40. D. Cairns, In: D. Cairns, editor. *Essentials of Pharmaceutical Chemistry*, 3<sup>rd</sup> ed, Pharmaceutical Press, London, 2008, Chapter 3.
41. *Zetasizer Nano User Manual*. Worcestershire: Malvern Instruments Ltd.; 2013.
42. A. Jintapattanakit, T. Kissel and V. B. Junyaprasert, *Mahidol Univ J Pharm Sci*, 35(1-4) (2008) 1.

43. W. Meng, T. L. Parker, P. Kallinteri, D. A. Walker, S. Higgins, G. A. Hutcheon and M. C. Garnett, *J Controlled Release*, 116(3) (2006) 314.
44. P. T. Wong and S. K. Choi, *Int J Mol Sci*, 16(1) (2015) 1772.
45. T. P. Thomas, B. Huang, S. K. Choi, J. E. Silpe, A. Kotlyar, A. M. Desai, H. Zong, J. Gam, M. Joice and J. R. Baker, *Mol Pharm*, 9(9) (2012) 2669.
46. W. Meng, M. C. Garnett, D. A. Walker and T. L. Parker, *Exp Biol Med (Maywood)*, 241(5) (2016) 466.
47. M. Vinci, S. Gowan, F. Boxall, L. Patterson, M. Zimmermann, W. Court, C. Lomas, M. Mendiola, D. Hardisson and S. A. Eccles, *BMC Biol*, 10(1) (2012) 29.
48. J. Friedrich, C. Seidel, R. Ebner and L. A. Kunz-Schughart, *Nat Protoc*, 4(3) (2009) 309.
49. J. Wang and G. Li, *Oncol Lett*, 9(2) (2015) 940.
50. S.-A. Yoon, J. R. Choi, J.-O. Kim, J.-Y. Shin, X. Zhang and J.-H. Kang, *Cancer Res Treat*, 42(3) (2010) 163.
51. J. G. Affleck, S. M. Nowickyj and V. K. Walker, *Cell Biol Toxicol*, 26(2) (2010) 117.
52. M. Serra, G. Reverter-Branchat, D. Maurici, S. Benini, J. N. Shen, T. Chano, C. M. Hattinger, M. C. Manara, M. Pasello, K. Scotlandi and P. Picci, *Ann Oncol*, 15(1) (2004) 151.

### Figure and table captions

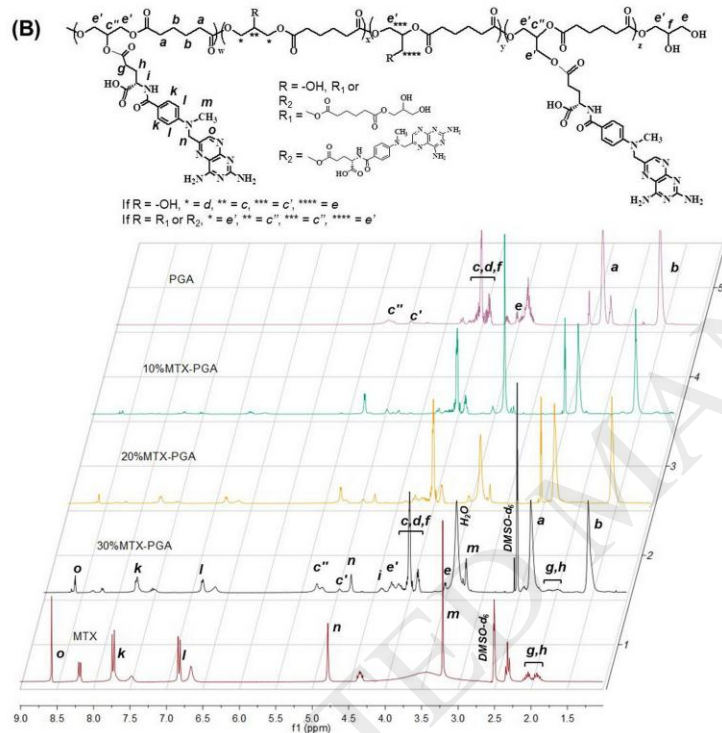
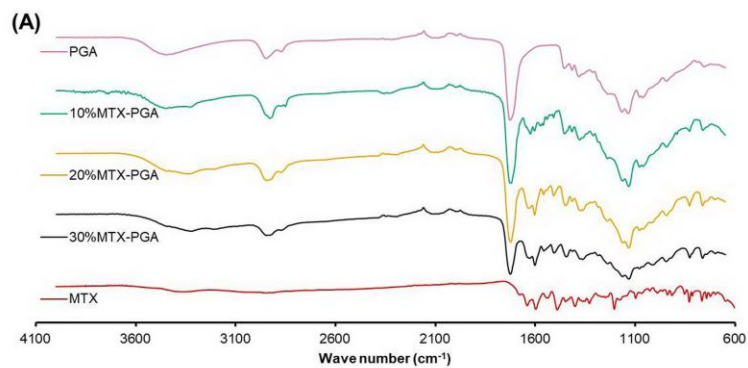
**Figure 1.** IR-ATR spectra (A) and  $^1\text{H}$  NMR spectra (B) of PGA, MTX and MTX-PGA conjugates.

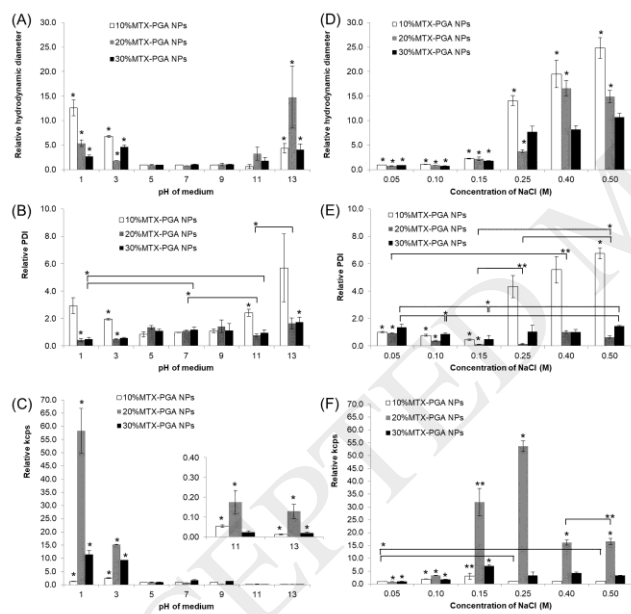
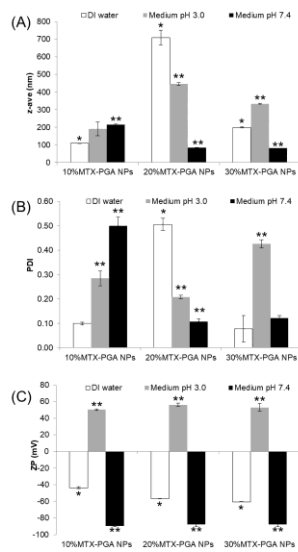
**Figure 2.** Mean hydrodynamic diameter (z-ave, A), size distribution (PDI, B) and zeta potential (ZP, C) of MTX-PGA NPs at various %MTX conjugations. An error bar indicates the standard deviation from three measurements. \*Statistically significant difference comparing different amount of conjugated MTX ( $p$ -value $<0.05$ ). \*\*Statistically significant difference compared to MTX-PGA NPs prepared in DI water at an equal amount of conjugated MTX ( $p$ -value $<0.05$ ).

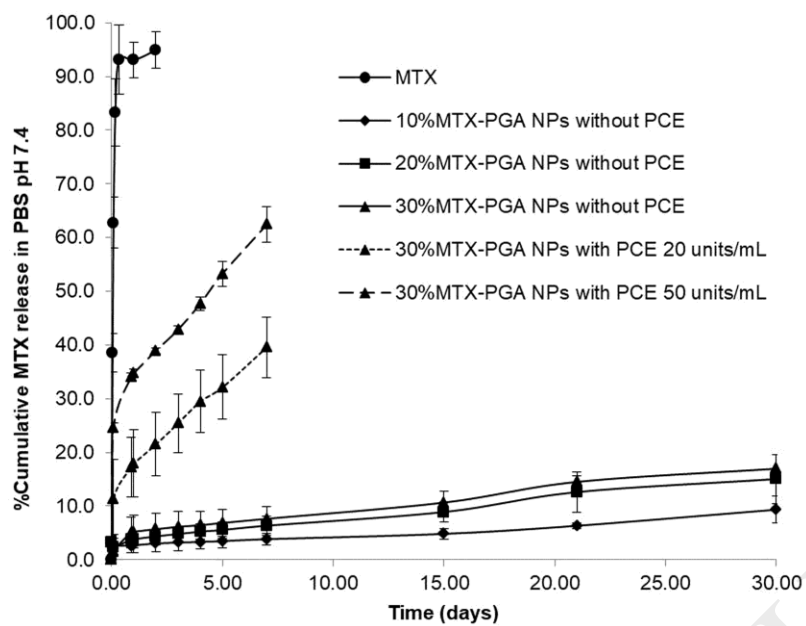
**Figure 3.** Relative hydrodynamic diameter (A and D), PDI (B and E) and  $k_{\text{pccs}}$  (C and F) of MTX-PGA NPs in various pHs (left column) and ionic strengths (right column) of media as compared to those in an equal dilution in sterile water for injection. Error bar indicates standard deviation of three measurements. \*Statistically significant difference when comparing the same formulation in different media ( $p$ -value $<0.05$ ). \*\*Insignificant difference when comparing the same formulation in different media ( $p$ -value $>0.05$ ).

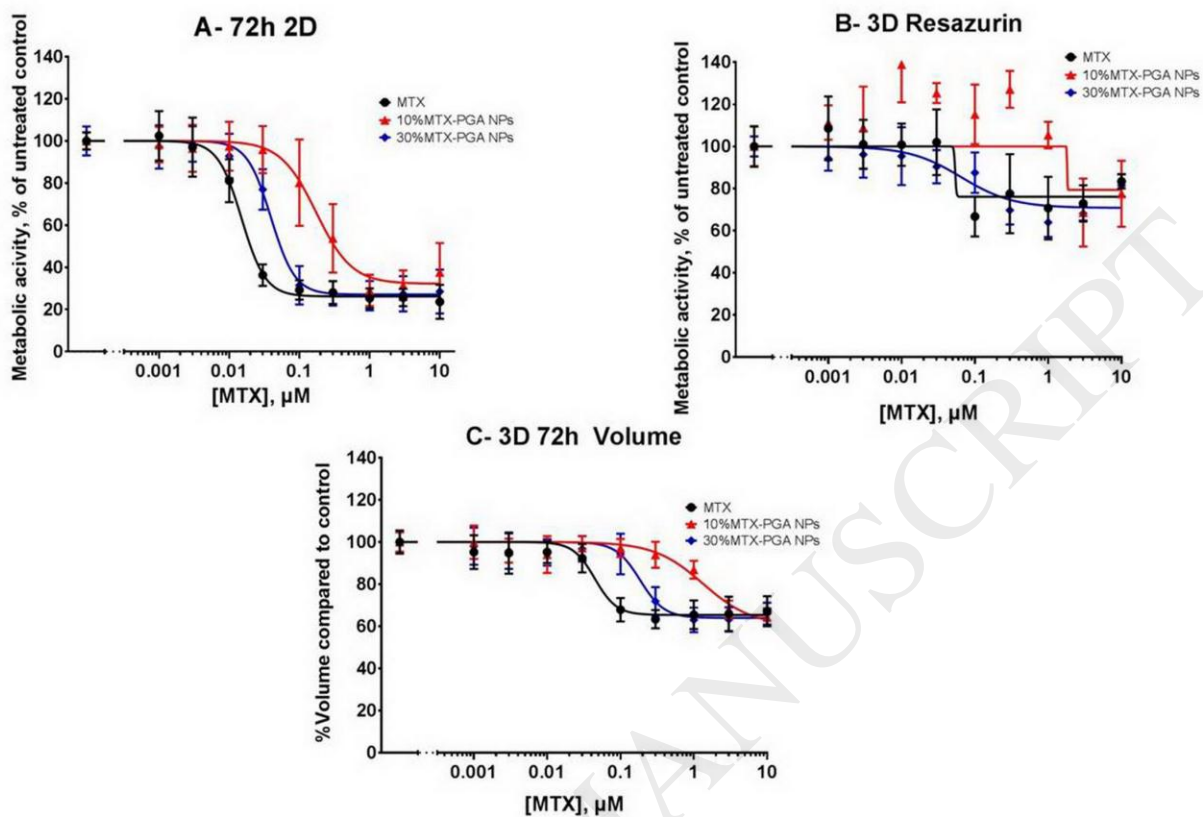
**Figure 4.** Release profiles of MTX from MTX-PGA NPs in PBS pH 7.4 with an absence of enzyme for 30 days and the presence of 20 and 50 units/mL PCE at 37°C for 7 days. Error bars indicate standard deviation from three experiments.

**Figure 5.** Viability of 791T monolayers and spheroids treated with MTX and MTX-PGA NPs for 3 days. A-resazurin viability assay for 791T cells treated in monolayer, B-resazurin viability assay for 791T spheroids, C-dose-response curves for spheroid volume. D-table summarising the  $\text{IC}_{50}$  and maximum effect with the corresponding 95% confidence intervals for the estimates. MTX (black circles), 10%MTX-PGA NPs (red triangles) or 30%MTX-PGA (blue diamonds)









D

Formulation	Resazurin metabolism		Volume	
	IC50, nM (95%CI)	Bottom of curve % of control (95% CI)	IC50, nM (95%CI)	Bottom of curve % of control (95% CI)
2D MTX	15 (14 to 17)	26 (24 to 28)	-	-
2D 10%MTX-PGA NPs	170 (140 to 210)	32 (28 to 36)	-	-
2D 30%MTX-PGA NPs	39 (36 to 44)	27 (25 to 29)	-	-
3D MTX	54 (Very wide)	76 (Very wide)	45 (<1 to 55)	65 (63 to 67)
3D 10%MTX-PGA NPs	1800 (Very wide)	79 (Very wide)	1300 (97 to 3200)	60 (45 to 66)
3D 30%MTX-PGA NPs	65 (31 to 120)	71 (67 to 74)	180 (150 to 220)	64 (62 to 66)

**Table 1** Molecular characteristics of PGA and MTX-PGA polymers**Table 2** Comparison of relative efficacy of polymer-drug conjugates (PDC) with MTX**Table 1** Molecular characteristics of PGA and MTX-PGA polymers

Polymer	$M_{n,GPC}$	$M_w/M_n$	%mole MTX/mole of polymer repeating unit		Conjugation efficiency by NMR <sup>b</sup>
			NMR	UV	
10%MTX-PGA	14621	2.21	7.0	8.86±0.32	58.3%
20%MTX-PGA	16215	1.61	14.5	17.33±1.25	60.4%
30%MTX-PGA	18579	1.95	27.5	33.26±4.72	76.4%

<sup>a</sup>Not determined

<sup>b</sup>Conjugation efficiency =  $\frac{\%MTX_{NMR}}{\%MTX_{Theoretical}} \times 100$ ; where  $\%MTX_{Theoretical} =$

$\frac{Weight\ of\ PGA}{MW_{glycerol\ adipate}} \times \%MTX_{Target} \times 1.2\ equiv.\ of\ DCC$ ;  $\%MTX_{NMR}$  is the %mole MTX

calculated by NMR per mole of polymer repeating unit,  $\%MTX_{Theoretical}$  is the theoretical %mole MTX per mole of PGA repeating unit, and  $\%MTX_{Target}$  is the target %mole of MTX per mole of PGA repeating unit and equals to 10, 20, and 30 for 10%, 20%, and 30%MTX-PGA, respectively.

**Table 2** Comparison of relative efficacy of polymer-drug conjugates (PDC) with MTX

PDC/MTX	791T cells		Saos-2 cells	
	IC <sub>50</sub>	IC <sub>50</sub> ratio of PDC/MTX	IC <sub>50</sub>	IC <sub>50</sub> ratio of PDC/MTX
<b>HSA-MTX experiment</b>				
MTX <sup>a</sup>	29 nM	-	-	-
HSA-MTX (16%) <sup>a</sup>	10,900 nM	377	-	-
<b>MTX-PGA experiment</b>				
MTX	15 nM	-	210.9 μM	-
10%MTX-PGA	170 nM	11.3	26.8 μM	0.127
30%MTX-PGA	39 nM	2.6	20.2 μM	0.096

<sup>a</sup>Data extracted from Garnett et al [4].